J. Phycol. **49,** 489–501 (2013)

DOI: 10.1111/jpy.12056

ALGAL TURF SCRUBBER (ATS) FLOWAYS ON THE GREAT WICOMICO RIVER, CHESAPEAKE BAY: PRODUCTIVITY, ALGAL COMMUNITY STRUCTURE, SUBSTRATE AND CHEMISTRY[1]

Walter H. Adey[2]*, H. Dail Laughinghouse IV*

Department of Botany, National Museum of Natural History, Smithsonian Institution, Washington, D.C., 20013, USA

John B. Miller

Chemistry Department – MS5413, Western Michigan University, Kalamazoo, Michigan 49008, USA

Lee-Ann C. Hayek

Statistics and Mathematics, National Museum of Natural History, Smithsonian Institution, Washington, D.C., 20560, USA

Jesse G. Thompson, Steven Bertman, Kristin Hampel, and Shanmugam Puvanendran

Chemistry Department – MS5413, Western Michigan University, Kalamazoo, Michigan 49008, USA

Two Algal Turf Scrubber (ATS) units were deployed on the Great Wicomico River (GWR) for 22 months to examine the role of substrate in increasing algal productivity and nutrient removal. The yearly mean productivity of flat ATS screens was 15.4 $g \cdot m^{-2} \cdot d^{-1}$. This was elevated to 39.6 $g \cdot m^{-2} \cdot d^{-1}$ with a three-dimensional (3-D) screen, and to 47.7 $g \cdot m^{-2} \cdot d^{-1}$ by avoiding high summer harvest temperatures. These methods enhanced nutrient removal (N, P) in algal biomass by 3.5 times. Eighty-six algal taxa (Ochrophyta [diatoms], Chlorophyta [green algae], and Cyanobacteria [blue–green algae]) self-seeded from the GWR and demonstrated yearly cycling. Silica (SiO_2) content of the algal biomass ranged from 30% to 50% of total biomass; phosphorus, nitrogen, and carbon content of the total algal biomass ranged from 0.15% to 0.21%, 2.13% to 2.89%, and 20.0% to 25.7%, respectively. Carbohydrate content (at 10%–25% of AFDM) was dominated by glucose. Lipids (fatty acid methyl ester; FAMEs) ranged widely from 0.5% to 9% AFDM, with Omega-3 fatty acids a consistent component. Mathematical modeling of algal productivity as a function of temperature, light, and substrate showed a proportionality of 4:3:3, respectively. Under landscape ATS operation, substrate manipulation provides a considerable opportunity to increase ATS productivity, water quality amelioration, and biomass coproduction for fertilizers, fermentation energy, and omega-3 products. Based on the 3-D productivity and algal chemical composition demonstrated, ATS systems used for nonpoint source water treatment can produce ethanol (butanol) at 5.8× per unit area of corn, and biodiesel at 12.0× per unit area of soy beans (agricultural production US).

Key index words: **Algal Turf Scrubber®; biochemistry; nutrient removal; productivity enhancement; species composition**

***Abbreviations*: 2-D, two-dimensional; 3-D, three-dimensional; ATS™, Algal Turf Scrubber; DHA, docosahexaenoic acid; EPA, eicosapentaenoic acid; FAMEs, fatty acid methyl esters; GC, gas chromatograph; GWR, Great Wicomico River; HDPE, high density polyethylene; ICP-OES, inductively coupled plasma optical emission spectroscopy; MSD, mass selective detector; PUFA's, polyunsaturated fatty acids**

The Algal Turf Scrubber (ATS) is an ecologically engineered, floway system for utilizing algal photosynthesis to control a wide variety of water quality parameters. Developed in the early 1980s at the Smithsonian Institution as a biomimicry of coral reef primary productivity, ATS was initially used as a tool to manage an extensive series of living microcosm and mesocosm models of wild ecosystems (Adey and Loveland 2007). Applied to closed living models, ATS units functioned to control nutrients, oxygen levels, carbonate systems, including calcification (through CO_2 control) and to minimize toxic compounds from the local human-engineered environment. ATS also allowed the development of planktonic communities and water borne reproduction in model ecosystems, as it has little effect on the planktonic component.

Algal Turf Scrubber was successfully scaled-up by HydroMentia, Inc. for nutrient removal from point-source and semi point-source open waters during the 1990s and early 21st century. ATS use ranged from aquaculture and tertiary treatment of sewage to agricultural canal amelioration of nutrients (Adey et al. 2011). By 2007, eight scaled-up ATS systems

[1]Received 28 June 2012. Accepted 13 December 2012.
[2]Author for correspondence: e-mail: adeyw@si.edu.
Editorial Responsibility: A. Buschmann (Associate Editor)

had been built and operated from coast to coast, mostly in the southern tier of states, including a 2.83 ha Tilapia operation in Falls City, Texas, that produced commercial quantities of fish for 9 years, and a 0.1 ha, ~950,000 $L \cdot d^{-1}$ tertiary sewage system in the northern Central Valley of California (Craggs et al. 1996). The ATS process has been used for water quality amelioration in a wide variety of environments and some of the earlier projects provided water quality analyses (Craggs et al. 1996, Stewart 2006). However, broad-based analytical studies, have been lacking, especially those that could allow the assessment of byproduct utilization of biomass.

Earlier non-point source work with ATS, had concentrated on the cleaning of environments rich in either hard benthic substrates (i.e., rock or branches) with abundant algal turfs as biofilms, or aquatic flowering plants that contained periphyton, epiphytically, on their stems. Those ATS systems were highly dominated by filamentous chlorophytes, particularly species of the genera *Cladophora, Spirogyra, Microspora, Ulothrix*, and *Rhizoclonium*. Diatoms and cyanobacteria were usually present, especially as epiphytes, but rarely provided significant biomass (Adey et al. 1993, Craggs et al. 1996). Later work on larger water bodies showed a greater dominance of diatoms and very high levels of species diversity, but generally lower productivity, as some filamentous diatoms tended to shear-off the floways before harvest (Sandefur et al. 2011, Laughinghouse 2012).

Algal Turf Scrubber was developed as a simple continuous flow low-cost means of utilizing algal photosynthetic and productivity potential using attached algae. Algal harvest and water/algal separation can be easily accomplished by suspending water flow and allowing the system to drain by gravity, since the algae are attached to the substrate. A wide variety of scraping and vacuuming methods apply. When nutrients are moderately high and solar energy moderately abundant, productivities ranging from 25 to 45 $g \cdot m^{-2} \cdot d^{-1}$ were common on ATS systems (Adey and Loveland 2007, Mulbry et al. 2008, Adey et al. 2011). The combined use of ATS to reclaim nutrients from eutrophic waters and to produce algal biomass coproducts, such as biofuels, soil amendments, or high-value extracts, reduces the costs of both processes. Equally important, the costs of algal production using ATS can be considerably lower than photobioreactor methods (Adey et al. 2011).

As a cohort of living organisms, including lesser amounts of bacteria, protists, and small invertebrates, the algal turf communities of ATS systems contain varying quantities of compounds essential to life: carbohydrates, lipids, proteins, genetic materials, structural components like silica, and a plethora of other organic and inorganic substances. It is known that individual species have different carbon (C), nitrogen (N), phosphorus (P), and silicon dioxide (SiO_2) bioaccumulation rates (Cade-Menun and Paytan 2010) as well as unique responses to light and temperature (Hessen et al. 2002, Wang and Lan 2011). Algal turfs can also contain extracellular materials, including terrigenous sediments. In this study, we analyzed the as-harvested algal turf biomass as a whole, rather than an analysis of individual species.

A large range of macro- and micro-algal species have rigid carbohydrate-based cell walls containing large quantities of simple and complex carbohydrates (Noseda et al. 1999). The structural carbohydrate composition of the diverse algal species may vary as the amount of sunlight, nutrients, and harvesting periods also change (Imbs et al. 2009, Skriptsova et al. 2010). Moreover, a large subset of algal species, particularly the Chlorophyta, uses carbohydrates as storage compounds (Raven and Beardall 2003). Regardless of biological function, if the carbohydrates can be liberated from the algal biomass the potential exists to produce bio-alcohols (ethanol and butanol) through fermentation (Potts et al. 2011, Wang and Lan 2011). The specific advantages of developing algae as a feedstock for bio -alcohol production include the following: nutrient absorption from eutrophic waters, oxygen injection into those waters, negligible competition with terrestrial agricultural starch or sugar crops for valuable arable land, a high growth-rate, and the potential for carbon dioxide absorption (Singh and Olsen 2011). Algal lipids have been studied extensively as a source for biodiesel production (Chisti 2007). However, some algal lipids have greater value in nonfuel products. Polyunsaturated fatty acids (PUFAs) are a component of the lipid profile in algae. This compound class, especially the omega-3 fatty acids, appears essential for human health. Algae are a potential alternative source to fish oil for essential fatty acids (Cequier-Sánchez et al. 2008, Inhamuns and Franco 2008). This article presents the productivity, community structure and chemical analyses of algal biomass produced from ATS floways on the Great Wicomico River (GWR) near Reedville, Virginia. In addition, we investigated the role of algal growth substrate in controlling ATS production and the relative effects of temperature and light.

METHODS

The GWR is a small tributary that lacks significant fresh water input, located on the west-central shore of the Chesapeake Bay, Virginia. It is mesohaline in character, with yearly salinity ranging from 11 to 18. The experiments were carried out on a 70 m long dock located on a 1 km wide embayment, about 6 km from the open Chesapeake Bay (Fig. 1). During this study, a semidiurnal tidal current (0.1 kn maximum) flowed perpendicular to the dock's axis. The ATS Floways (#1 and #2) were 0.61 m wide fiberglass troughs, with 15.2 m length (1% slope) and 24.4 m length (2% slope), respectively.

The floways had oscillating input trays (Fig. S1, see Supporting Information) that provided a surging motion in the water column moving down the floway (Carpenter et al.

FIG. 1. Floway #1 (left) and Floway # 2 (right) on the Great Wicomico River off the Central Chesapeake Bay.

1991, Adey and Loveland 2007). Two submerged centrifugal pumps (38 L · min^{-1} flow) were installed on each floway and placed on the outer part of the dock, with separate PVC pipe lines (24.4 m long, #1; 15.2 m long, #2) leading to the oscillating input trays. The pumps were placed on separate electrical circuits and had an automatic backup electrical generator in the event of failure of the commercial power source. Interruption of water flow occurred only during short-term non-drying harvests over the 22 months of floway operation. This is a critical element of ATS operation, since 4–6 weeks is typically required to build a mature, fully productive community of algae (Fig. S2, see Supporting Information).

Water samples were taken on several occasions in both autumn and spring for analysis of nitrogen and phosphorus, and the samples were collected from the river near the pump intakes and on the inflow and outflow of both floways. Samples were taken directly in 500 mL acid-washed plastic bottles and frozen shortly after collection. Analyses were carried out by the water quality laboratory at the Virginia Institute of Marine Science. Water temperature and pH were measured by hand with a Hanna Instruments HI 9024 microcomputer/pH meter. Readings were taken weekly or bi-weekly, before harvest at the river input and in the incoming and outflowing water on the floways, and occasionally every two h from 0600 to 2200.

The two floways were studied from August 2009 to June 2011 (22 months). On Floway #1, tests were carried out on algal growth and dynamics relative to different substrate types, with an emphasis on comparing the traditional two-dimensional (2-D) design to a variety of three-dimensional (3-D) designs (Fig. S3, see Supporting Information). Growth experiments on Floway #2 were primarily focused on measuring productivity on a single type of 3-D screen prototype developed after the initial Floway #1 studies showed a strong increase in production on some 3-D types. In addition, two short-term experiments on CO_2 introduction and lipid triggers were undertaken on Floway #2 and will be described fully elsewhere. All algal settlement on the floways "self-seeded" from the GWR water and no filters were employed.

Floway #1. The traditional substrate in the ATS system is a flat plastic screen. An HDPE screen of 3 × 5 mm mesh is typical, although a wide range of mesh sizes and screen materials have been tested. On the scale of the ATS floway and the attached algal community, these screens are 2-D structures. The dominant diatom communities that occurred on Chesapeake ATS systems quickly attach to these "standard" screens, but depending on the species, their filaments/chains can constantly "shear-off" in the moderate energy environment of an ATS, producing a lower standing crop and ultimately lower water remediation capabilities and biomass accumulation than communities higher in filamentous green algae.

This experiment was established primarily to determine how to prevent the loss of fragile diatom filaments, and principally involved examining the efficacy of 3-D screens/fabrics as support structures. A wide variety of off-the-shelf, deep pile throw rugs, with 1–2 cm thick loose fibers, were tested along with special, more open variants produced for this project by the carpet company InterfaceFLOR (La Grange, GA, USA). Multiple layers of 2-D screens, and open plastic fabrics used for soil retention were also examined. Most provided some improvement in diatom retention over simple 2-D screens, but unfortunately were readily degraded by solar UV. Several screens were hand woven, with the specific purpose of structuring a growth environment with the limitations of diatoms in mind. Braided Dacron fibers (2 cm long) were attached to a 5 mm mesh basal screen (Fig. S3). The Dacron was employed because it would provide for minimal degradation by solar UV. The braided fibers were used to provide maximum attachment surface for the diatoms. Two types, one with a coarser braid (labeled #14) and the other with a fine, "hairy" surface (labeled #17) were used. These were established in the central part of the ATS test floway. Standard 2-D and other 3-D ATS screens were arrayed both above and below for comparison.

Sampling of test screens, and whole floway harvest were generally performed every 7 d in the summer and 14 d in the winter. Depending on the treatment, sample size on Floway #1 varied from 0.13 to 0.14 m^2; the standard sample size on Floway #2 was 0.14 m^2. There was a small amount of variation in harvest period due to weather and during the spring and fall when switchover occurred from one harvest schedule to the other. On the day of harvest, water flow on the ATS floway was stopped and the system was allowed to drain for one half to 1 h, depending on humidity and temperature. At no time was the floway allowed to fully dry, as it was essential not to reduce the viability of the ("seed") algal community remaining on the floway after harvest. Harvest of all test screens, and the intervening 2-D screen that extended down the whole floway, was achieved by hand with a small wet-dry shop vacuum. While the vacuum severs and removes the predominance of the algae on the growing screen surface, delivering the biomass to the storage chamber of the shop vacuum, a basal layer of short algal filaments remains attached to the floway screens to quickly re-initiate growth.

Each test sample was more fully drained on coarse and fine filters immediately after harvest, and the samples and their filters dried at 50°C–55°C in an Excalibur Food Dehydrator (Excalibur, USA) until weight was stable for 6 h (typically 48–72 h total drying). The final dry weight was recorded at ±0.1 g and the samples stored, in plastic containers at 10°C–12°C, for future reference. The wet, bulk sample of whole floway harvest (about one half of the floway surface, with 2-D screen) was placed in plastic 20 L buckets from which several separate aliquots, each taken after stirring, were extracted and placed in one liter glass, food-storage jars and immediately placed in a freezer.

Starting in the 11th month of Floway #1 operation (July 2010), several aliquots were taken from the bulk sample,

before freezing, for algal species analysis, placed in plastic sample bags and kept refrigerated until analysis. At that time, poorly performing 3-D screens were also removed, leaving a substrate of 2-D screen on much of the bed of the floway for the remainder of the experiment. Since the 3-D screens were sampled before the whole floway harvest and the bulk sample taken, 80%–90% of Floway #1 biomass was provided from 2-D screens.

Floway #2. The 3-D substrate used on Floway #2 was coarser than the "optimal" hand-woven 3-D substrates on Floway #1 (#14 and #17, Fig. S3). This was produced by the carpet company InterfaceFLOR to examine the possibility of large-scale 3-D screen production. Algal biomass accumulation on the Floway #2 substrate (both on the smaller samples in Floway #1 and on the whole Floway of #2) was about two-thirds that of the optimal screens (#17, #14, 3-D) for the same 12-month period (see Results). Floway #2 was not fully operational until summer 2010, and the lack of funding required a shutdown early in the summer of 2011. Thus, a full data set was not available for the highly productive summer interval. However, Floway #2 provided the critical analysis of a 3-D screen growth substrate as applied to a whole floway unit, rather than the smaller individual sample screens.

Algal species analyses. Random aliquots from the bulk sample were homogenized and a 5 mL subsample was blended with water to a 400 mL final concentration. A subsample of 100 mL was separated and standard Lugol's solution was added to sediment the sample; it was allowed to stabilize in preparation for quantitative analyses. Identification to lowest taxonomic level possible and relative abundance counts were conducted using a Zeiss inverted microscope (Zeiss, Oberkochen, Germany) at 400×, following the Utermöhl procedure (Utermöhl 1958). Samples are maintained in a liquid herbarium in Rm. E-117 at the National Museum of Natural History, Smithsonian Institution, Washington, D.C., USA.

Algal chemical analyses. Analytical methods: Sources and preparation of the materials, reagents, and samples used for chemical analysis of the ATS biomass are described in Appendix S1, in the Supporting Information.

Ash analysis: The weight percent ash in each algal sample ($g_{ash} \cdot g_{algae}^{-1}$) was determined according to the method ASTM E 1755 2007 (ASTM, 2007 #27).

Nutrient analysis: Carbon, hydrogen, and nitrogen content of algal samples was analyzed using a Leco Corporation Truespec® CHN analyzer. Lyophilized algae were oven-dried at 105°C for one h and stored in a desiccator prior to analysis. The instrument was calibrated before each set of analyses using an EDTA standard and blank checks were run between every 10 and 15 analyses. Triplicate measurements were made for all samples.

Total phosphorus levels of algal samples were determined by a digestion and colorimetric method (Dick and Tabatabai 1977). Lyophilized algae (0.03–0.08 g) were digested in a solution of 2 M sodium hydroxide and liquid bromine at 250°C, heating to dryness. The samples were then reconstituted with formic acid and 0.5 M H_2SO_4 and analyzed by colorimetry using a Perkin Elmer Lambda Bio 20 spectrophotometer at $\lambda max = 711$ nm. Triplicate measurements were made for all samples.

The total silicon of algal samples was measured by a modified literature method (Reay and Bennett 1987). Briefly, a solution of potassium tetraborate and potassium nitrate was heated at 100°C in clean oxidized nickel crucibles, until completely evaporated, then cooled to ambient temperature. A weighed portion (25–50 mg) lyophilized algae was added to the crucibles and heated in air at 300°C for 2 h. Solid potassium hydroxide (0.4 g) was added to each crucible, heated until molten (~>410°C) and held at temperature for 30 min. After cooling, the soluble residue was extracted with 20 mL of water and centrifuged. Aliquots of the supernatant were analyzed by inductively coupled plasma optical emission spectroscopy (Perkin Elmer Optima 2100DV ICP-OES). Triplicate digestions were performed for each biomass sample and triplicate measurements made for all digestions. Total SiO_2 was calculated from the total silicon, which presumed no other significant silicon compounds.

The proportion of biogenic silica was determined using a time-digestion procedure modified from that of Conley and Schelske (1993). Briefly, algal biomass (30–50 mg) was weighed into six 50 mL polypropylene centrifuge tubes, to each of which was added 40 mL of 5 wt.% sodium carbonate solution. All but one of the tubes was heated to 70°C under continuous stirring. A 1 mL aliquot was removed from the unheated tube immediately, and at intervals (1, 2, 3, 4, 5, and 24 h) a 1 mL aliquot was taken from a previously un-sampled heated tube. The sodium carbonate in each of the sampled aliquots was quenched immediately with 5% nitric acid. The acidified samples were diluted and analyzed by ICP-OES. The proportion of silica that is biogenic was determined by performing a linear fit of the silicon in solution versus digestion time for times longer than 2 h; the biogenic silicon is the y-intercept of the fitted line, as described in the literature method.

Carbohydrate analysis: Preparation of the ATS algal biomass for carbohydrate analysis was a three-step process: (i) hydrolysis with strong acid to convert all carbohydrates to their constituent monosaccharides, (ii) reduction of the monosaccharides to their corresponding alditols, and (iii) derivatization of the monosaccharide hydroxyls with acetyl groups. The derivatized carbohydrates were identified and quantified by Gas Chromatography Mass Spectrometry (GC-MS) analysis.

Lipid analysis: Fatty-acid based lipids from the lyophilized algae samples were converted to the corresponding fatty acid methyl esters (FAMEs) and analyzed by gas chromatography (GC). Reporting fatty-acid based lipids on a FAMEs basis leads to a systematic underestimate of somewhat less than 1% in the absolute quantity for triglyceride lipids, and a systematic overestimate of 3%–4% for any phospholipids. However, these systematic deviations are generally small compared to the variability in the overall analytical method.

Modeling of productivity. In this study, we also analyzed primary productivity as a function of light and temperature. Light data were derived from NASA monthly predictions for Annapolis, MD; Washington, D.C.; and Charlotte, NC. The mean of these three data sets was equally matched against the Smithsonian Institution SERC Laboratory daily light data for the Rhode River, MD, just south of Annapolis. Temperature data were taken on site, as presented above.

RESULTS

Temperature and pH. Out-flowing water temperature changed little from river temperature on these floways, although atmospheric temperature extremes were observed as brief deviations of the discharge temperature when compared to the river temperature (Fig. S4, see Supporting Information). River and floway incoming water had a mean yearly pH of 8.25 (SD 0.15). At night, there was little change in pH, however, through mid-day (0900–1500 h), pH rose uniformly down Floway #2, reaching 8.5 (SD 0.24) by the middle of the floway and 8.64 (SD 0.15) at the effluent, as CO_2 was extracted from the water column by algal photosynthesis.

TABLE 1. Mean nutrient (N, P) levels in the Great Wicomico River and in the outflow of Floways #1 & #2 during Fall 2010 and Spring 2011 in mg · L^{-1}.

Fall 2010 mg · L^{-1}	River	Outflow Floway #1	Outflow Floway #2	Spring 2011 mg · L^{-1}	River	Outflow Floway #1	Outflow Floway #2
PN	0.1008	0.0683	0.0447	PN	0.239	0.134	0.079
PP	0.0066	0.0038	0.0023	PP	0.0126	0.006	0.0012
TDN	0.3234	0.2783	0.2442	TDN	0.3536	0.3493	0.3176
TDP	0.0095	0.007	0.0054	TDP	0.015	0.009	0.0059
TN	0.4242	0.3466	0.2889	TN	0.5926	0.4833	0.3966
TP	0.0161	0.0108	0.0077	TP	0.0276	0.015	0.0071
	Six sampling periods of two samples each				Five sampling periods of two samples each		

PN, particulate nitrogen; PP, particulate phosphorus; TDN, total dissolved nitrogen; TDP, total dissolved phosphorus.
Each number represents 12 weekly samples (Fall 2010) and five weekly samples (Spring 2011). See text for statistical analysis.

Nutrients. The GWR had moderate nutrient levels during both fall and spring (Table 1), and these levels were not likely limiting for the production levels seen on the screens of Floway #1. By paired sample *t*-test, TN ($t_{50} = -2.245$, $P < 0.029$) and TP ($t_{50} = -3.322$, $P < 0.002$) were both significantly reduced between river source water and floway effluent. The significant TP reduction highly was due to phosphorus precipitation with elevated pH. In the analysis of the harvested biomass, no effort was made to distinguish between extracellular and intracellular phosphorus.

Productivity floway #1. The 3-D screens showed a consistently greater level of algal biomass than the 2-D screen with summer production about five times that of mid-winter production on both types of growth substrate ($t_{68} = 5.959$, $P < 0.001$; Fig. 2). Largely following temperature and light, the 3-D screens produced at a level of about 2.5 times that of the 2-D screens; the yearly mean for both 3-D screens combined was 36.9 g · m^{-2} · d^{-1}, and that for the combined 2-D screens was 15.4 g · m^{-2} · d^{-1}. Separate analysis of the 3-D screens showed that production on the two screens followed each other closely. However, the screen with the finely braided and somewhat hairy surface produced biomass 15%–20% higher than the screen with the coarser fibers. The difference was relatively small, but highly significant ($t_{68} = 10.893$, $P \leq 0.0001$), even though the two screens were situated only one meter apart on the floway. Three-dimensional screen #17 was placed downstream of 3-D screen #14, and 3-D screen #17 appeared to be at a disadvantage for production due to lesser nutrients and suspended particulates. Biomass productivity on 2-D screens placed at about the 10% and 80% positions on Floway #1 followed each other closely over the entire period of study and there was no significant difference in production between the two positions ($t_{64} = -1.189$).

Floway #2. The primary difference between the two floways was the addition of 3-D substrate on the entire length of Floway #2 (Fig. 1). The hand-woven 3-D substrates described above (Fig. S3) were nearly three times as productive as the flat screens used in previous studies. However, the only 3-D substrate

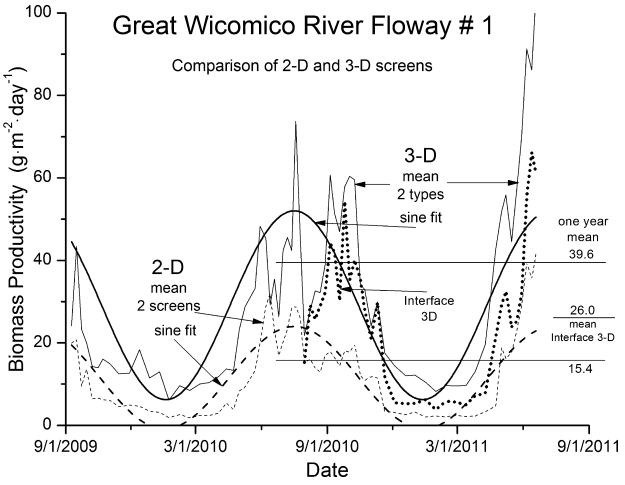

FIG. 2. Biomass productivity on Floway #1, comparing 2-D (dashed lines), 3-D (solid lines) and Interface (bold dotted line) growth substrate (screens). The smooth curves are sine functions fit to the two data sets. Note the one-year mean production marked for the different screen types.

available in large quantity at the time of construction was one of the InterfaceFLOR types being tested on Floway #1. We understood the characteristics of this screen and how it related to highly productive hand-woven type 3-D substrates (Fig. 2); however, that information was only available as test rectangles. This was the first time that 3-D screens had been employed in an environment rich in diatoms and it was essential that we understood how the 3-D substrate would perform on whole floways.

The manufactured 3-D screen used in Floway #2, when deployed as a test square in Floway #1, produced biomass at approximately 67% of the optimum 3-D screens (Fig. 2). This was the mean of the manufactured types; the optimum manufactured screen used on Floway #2 performed at a 13% higher level. Thus, we would have expected the upper part of Floway #2 to perform at about 80% of its hand-woven 3-D equivalent. On the upper half of Floway #2, during August and September, the manufactured screen produced at 40–50 g · m^{-2} · d^{-1}, while on floway #1, the 3-D screens were producing at 60–70 g · m^{-2} · d^{-1} and the 2-D screens at 20–30 g · m^{-2} · d^{-1}. Therefore, 3-D screens can

significantly increase biomass production on long floways as well as on small test screens, but to achieve optimum production the right screen configuration is necessary.

Algal biodiversity. Floway #1: A total of 86 algal taxa belonging to seven different phyla dominated by Ochrophyta (54%), Chlorophyta (24%), and Cyanobacteria (22%) were found on this system (Rhodophyta and Dinophyta provided less than 1% of the flora). The most diverse phylum was Ochrophyta (diatoms) with 78% of the total taxa (67 of 86 taxa) coming from this group. Ochrophyta was also the most abundant algal group on the system during the study period 54% of total relative abundance. The most abundant taxa were *Berkeleya* spp. (*B. fennica* Juhlin-Dannfelt, *B. fragilis* Greville, and *B. rutilans* (Trentepohl ex Roth) Grunow; 20%), *Gloeothece* sp. (13%), *Ulva intestinalis* Linnaeus (10%), *Ulothrix* sp. (9%), *Melosira* spp. (*M. monoliformis* (O. F. Müller) C. Agardh and *M. nummuloides* C. Agardh; 9%), *Lyngbya salina* Gomont (7%), and *Achrochaete* sp. (7%). Other taxa occurring on the floway individually accounted for less than 2% of the total abundance. The most frequent taxa (>84%) were *Achnanthes* spp. (i.e., *Achnanthes brevipes* C. Agardh), *Amphora* spp., *B. rutilans, Mastogloia* spp., *M. nummuloides, Stauronella* sp., *Navicula* spp., and *Grammatophora* spp.

Periphyton growing on these engineered systems were dynamic (Fig. 3a). Diatoms were always present and abundant; different species dominanted seasonally. For example, *Tabularia tabulata* (C. Agardh) Snoeijs, *Nitzschia sigmoidea* (Nitzsch) W. Smith, and *N. sigma* (Kützing) W. Smith were most abundant from July to September, but were absent during colder months when other taxa, such as *Nitzschia nana* Grunow, *Thalassionema nitzschiodes* (Grunow) Mereschkowsky, and *Thalassiosira* sp., appeared. However, as a group, chlorophytes tended to increase during late spring through summer and reached 70% of total abundance for a short period in the spring. Cyanobacteria were abundant in fall due to the large amount of two taxa: first, in mid-September, *Gloeothece* sp. dominated the periphyton; later in the fall, *L. salina* dominated.

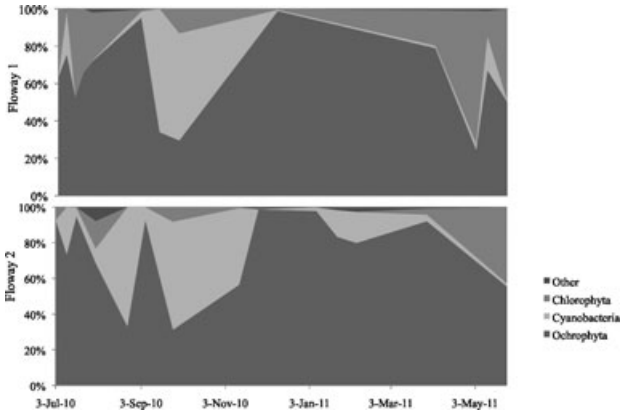

FIG. 3. Seasonal relative abundance of algal species, by phyla on Floways #1 (a – Upper) and Floway #2 (b – lower; July 2010 to June 2011).

Floway #2: On this floway, 98 algal taxa, belonging to seven different phyla dominated by Ochrophyta (68%), Chlorophyta (7%), and Cyanobacteria (24%) were found (Rhodophyta and Dinophyta together contributed 1% of the flora). The most diverse phylum was Ochrophyta (diatoms) with 74% of the total taxa (73 of 98 taxa) coming from this group, while also being the most abundant algal group on the system during the study period (68% of total relative abundance). Other phyla accounted for roughly 1% of total relative abundance. There were 7 taxa of dinoflagellates compared to only 2 taxa on Floway #l. The most frequent taxa (>85%) were *Achnanthes* spp. (i.e., *A. brevipes*), *Amphora* spp., *B. rutilans, Grammatophora* spp., *Licmophora* spp., *M. nummuloides*, *Navicula* spp., and *T. tabulata*. The most abundant taxa were *Berkeleya* spp. (*B. fennica* and *B. rutilans*; 19%), *Lyngbya cf. salina* (19%), *T. nitzschiodes* (14%), *M. nummuloides* (7%), and *U. intestinalis* (6%). The other taxa occurring on the floway accounted for 3% or less of total abundance each.

The periphytic community on Floway #2 was also seasonally dynamic (Fig. 3b). Diatoms were always present, though there were changes in community structure occurring throughout the year. Cyanobacteria increased from August to November (up to 60% of total abundance, dominated by *L. salina*). Although present several times during the year, chlorophytes peaked in abundance in late spring (40% of the total relative abundance); both *U. intestinalis* and *Ulothrix* spp. were responsible for this abundance.

Seasonality in species biomass and abundance was marked on both floways. While the beginning of the seasons were not exactly the same on the two floways, they were close enough to be regarded as system characteristics dependent on a mix of light and temperature. While both floways have the same sets of species, seasonally and in relative abundance, a few differences were marked. *Acrochaete* sp. and *Ulothrix* sp. were important summer and spring species on Floway #1, yet were unimportant on Floway #2; the diatom *Thalassionema nitzschiodes* was the dominant species in the winter on Floway #2, yet was virtually absent on Floway #1.

The side-by-side floways had the same water source, light, and temperature; yet had different screen types (2-D vs. 3-D) and algal productivities. The floways also differed in slope (Floway #1: 1%; Floway #2: 2%); the higher slope was added to Floway #2 to compensate for the effects of a rougher screen surface on water flow. With the continuous 3-D substrate on Floway #2, the diatoms *Berkeleya* and *Melosira* replaced the green alga *Ulva*, especially in spring and summer.

Algal turf biomass composition. *Nutrients (C, N, P, Si):* Algal biomass was harvested from upper and lower regions of Floway #1 and #2, at various times from October 2010 through May 2011. There was no clear seasonal trend in any of the C, N, and P of harvested biomass, although N was somewhat higher and C somewhat lower in late winter or early spring than in early summer (Fig. 4). On the basis of the Redfield ratio, we expected that the N, P, and C levels should be correlated; however, there was no correlation ($R^2 < 0.07$) between C and either N or P in the algal biomass. To provide an overall assessment of nutrient accumulation, each data set in Figure 4 was averaged; the mean values are collected in Table 2. The C content of the algal biomass from Floway #2 was somewhat higher than that from Floway #1, with lower Floway #2 biomass being higher in C than either Floway #1 or upper Floway #2 (Table 2); P and N content of lower floway #2 were also somewhat higher. Pair-wise comparisons between lower Floway #2 and Floway #1 showed that the differences were generally significant (Table 2).

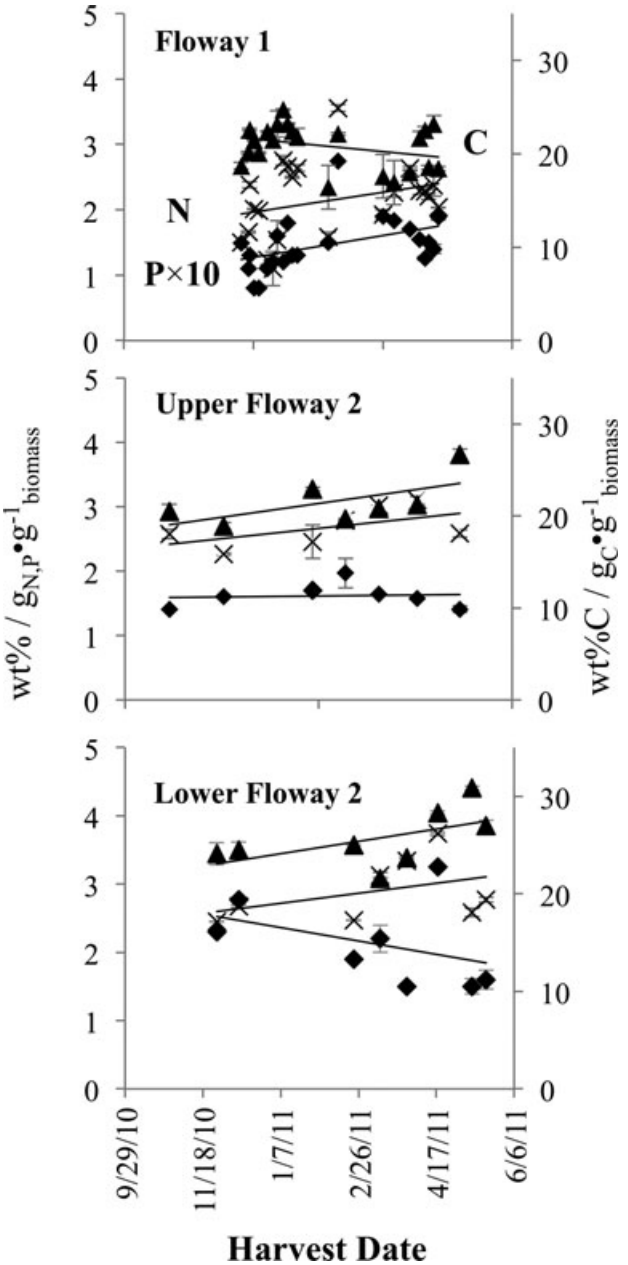

FIG. 4. Temporal variation in levels of carbon (triangles), nitrogen (crosses), and phosphorus (×10; diamonds) measured in algae from Floway 1 (**top**) upper Floway 2 (**middle**) and lower Floway 2 (**bottom**). Carbon is plotted on the secondary axis. Error bars represent the sample standard deviations of triplicate analyses. Lines are linear fits.

The total quantity of SiO_2 decreased during the late winter when the water temperature was cooler and terrestrial runoff events were less frequent. In any event, there was considerable variability in total SiO_2 (Table 3). The basic origin of SiO_2 in the harvested material was biogenic and terrigenous. The amount of biogenic SiO_2 was measured on two sample dates (23 February 2011 and 23 May 2011) with a mild, basic digestion (Table 3).

Algal turf carbohydrates. The carbohydrate content of the algal turf biomass was measured for a time series of samples from Floway #1 and upper and lower Floway #2, and also lacked a clear seasonal correlation (Fig. 5, a and b). In comparison to the population dynamics plots (Fig. 3, a and b), higher carbohydrate levels corresponded to higher proportions of Chlorophyta and Cyanobacteria in the turf community. It was also clear that the most abundant and variable monosaccharide component was glucose.

Fatty-acid lipids. Algae samples from Floway #1 and upper and lower Floway #2 were analyzed for overall fatty-acid based lipid content, especially the nutritionally important ω-3 polyunsaturated fatty acids eicosapentaenoic acid (EPA) and docosahexaenoic acid (DHA). The weight percentage of FAMEs on an AFDM basis ($g_{FAMEs} \cdot g_{AFDM}{}^{-1}$) showed similar temporal variation for all of the floways (Fig. 5c). By comparison with the relative phyla abundances (Fig. 3, a and b) higher lipid contents corresponded to higher proportions of Ochrophyta. EPA and DHA levels generally were correlated (Fig. 5, d and e), with EPA levels systematically higher than those of

TABLE 2. Overall mean carbon, nitrogen, and phosphorus composition of algal turf harvested from the Great Wicomico River ATS systems.

	Mean wt%/g · g^{-1}_{algae}		
	P	N	C
Floway 1	0.147 ± 0.051	2.125 ± 0.070	20.88 ± 2.36
Floway 2 (all)	0.177 ± 0.052	2.438 ± 0.590	22.22 ± 0.52
Upper Floway 2	0.162 ± 0.019	2.680 ± 0.301	21.53 ± 2.60
Lower Floway 2	0.213 ± 0.059	2.890 ± 0.463	25.67 ± 2.9

TABLE 3. Season variations in total and biogenic silica in algal turf harvested from the Great Wicomico River ATS systems.

	Mean wt%/g · g^{-1}_{algae}	
Harvest dates	Total SiO_2	Biogenic SiO_2
November–December	41.4(±6.2)	*a*
February–March	27.2(±4.0)	2.2(±2.0)
May–July	52.1(±4.5)	27.6(±2.3)

DHA. Curiously, PUFA levels did not correlate with variations in species distribution at the phyla level, as the overall lipid levels did. Instead, specific genera were more important contributors to the PUFA content, perhaps *Thalassionema* or *Berkeleya*.

Modeling of productivity. Algal production on the GWR test floways was a function of both light and temperature (Fig. 6). Mean production on 3-D (#17) screen substrate was consistently about 3× greater than that on the 2-D screens, as demonstrated earlier for the yearly mean. Algal production was related to temperature (Regression: $F_{1,52} = 131.272$, $P \leq 0.0001$) and light (Regression: $F_{1,52} = 74.921$, $P \leq 0.0001$); the regression line for temperature had a higher slope than for light, and production was more variable as a function of light than temperature. The higher variation likely resulted from the regional light database as compared to the on-site temperature data. The ratio of slopes between the two showed that temperature provides 61.5% of the total rise and light about 38.5%.

Temperature and light were mutually important on driving productivity (Fig. 7). To describe these data, we chose a linear model (eq. 1) after comparison with multiple polynomials because the linear equation fit with equal significance and provided equivalent predictive power. The model described the algal production on 3-D screen #17 as a combined function of temperature and light (T-L), where productivity P(T-L) had units of g · m^{-2} · d^{-1}, and T-L had units of °C-mol photons · d^{-1}.

$$P(T\text{-}L) = 9.05 + 0.04(T\text{-}L) \quad (1)$$

Equation 1 was used to estimate the "true" values of the six depressed data points in the plot of Figure 2 that we ascribed to excessive temperature excursions during harvest. The time-dependent productivity of the 3-D test screen #17 was plotted in Figure 8, with the six data points replaced by the estimated values. An empirical time-dependent productivity function P(*t*) derived from equation 1 and the Temperature-Light function was described by equation 2, where P(*t*), P_0 and P_t had units of g · m^{-2} · d^{-1}; *t* and t_0 had units of days; and ω had units of days radian^{-1}. The P_0 term was the average annual productivity, and has a value of 35 g · m^{-2} · d^{-1}, while P_t was the difference between the annual minimum (winter) and maximum (summer) productivity and had a value of 32 g · m^{-2} · d^{-1}. Together, eqs 1 and 2 empirically described the performance of the 3-D screen #17 growing surface.

$$P(t) = P_0 - P_t\sin(2\pi(t\text{-}t_0)/\omega) \quad (2)$$

DISCUSSION

Adey et al. (2011) reviewed the status of algal productivity as used in ecologically engineered systems to produce algal biomass and remove nutrients from waste waters, and they compared ATS systems to that of typical suspended microalgal production in bioreactors. The results of this study showed that providing 3-D substrate structure, extending above the traditional flat 2-D screen, significantly enhanced diatom retention in ATS systems and therefore biomass productivity. Enhanced productivity likely also resulted from the increase in attachment surface and the resulting higher density of chl and other photosynthetically active pigments. This was seen in the significantly improved productivity of the finer braided 3-D screen as compared to the coarser variety. However, some of the enhancement also lies in the physical disruption of laminar flow that diatom filament strength cannot tolerate. The surface character of the 3-D fibers needs to be further investigated, as major improvements in production seem likely with this parameter.

Biomass production rates during the summer of 2010 showed a series of dips that were not characteristic of ATS floways. In late August, the dips were observed and correlated to high harvest temperatures on the floways; the harvest mode was subsequently shifted from late-afternoon to early-morning and biomass production dips ceased. At the first dip, the incoming river water temperature was about 27°C. When the dips were finally prevented, the temperature was about 29°C, falling from a peak of nearly 34°C. Approximately, 1.5 h was required to harvest this floway; as described earlier, test screen sampling was carried out first, followed by a general floway harvest. A large part of the water on the floway was allowed to drain in this process to facilitate separation of the algal biomass from the entrained water. On very hot, sunny afternoons, the algae and remaining water likely exceed 50°C and these temperatures would be fatal to the remaining algal seed community. The high-temperature excursions during harvesting were likely responsible for the strong dips in biomass production during the summer of 2010.

During the late spring and early summer of 2011, all harvests took place in the early morning to minimize the influence of the sun warming a drying floway. Biomass harvests in early June 2011 on these 3-D screens had exceeded 90 g · m^{-2} · d^{-1} (Fig. 2);

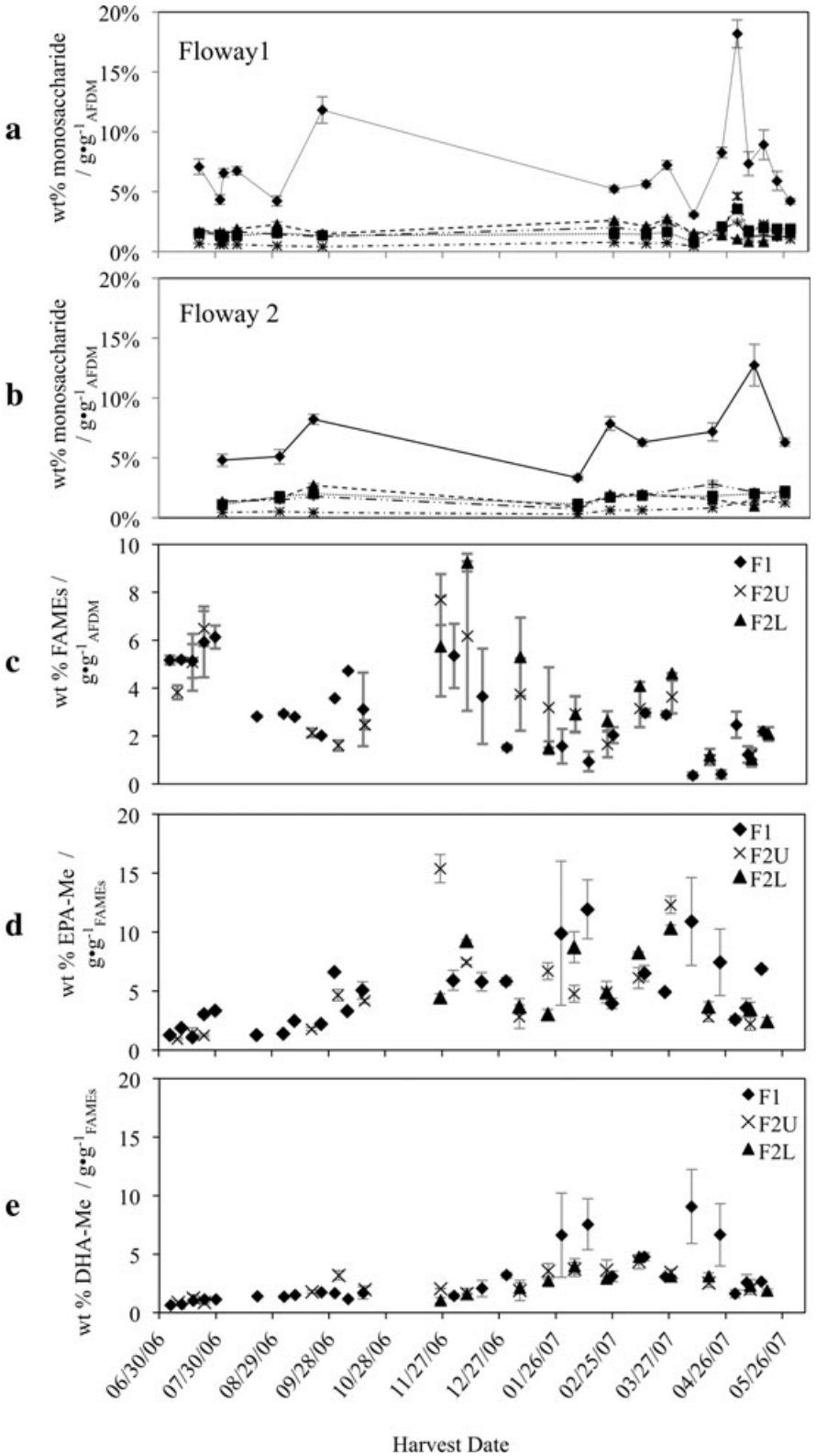

FIG. 5. (a and b) Temporal variation of total carbohydrates from the algae harvested from Floway #1 (F1-diamonds), upper Floway #2 (F2U-X), and lower Floway #2 (F2L-triangles). Error bars represent the sample standard deviations of replicate analyses. (c) Temporal variation of fatty acid lipids (as FAMEs) from the algae harvested from Floway #1 (F1-diamonds), upper Floway #2 (F2U-X), and lower Floway #2 (F2L-triangles). Error bars represent the sample standard deviations of replicate derivatizations. (d and e) Temporal variation of (top) EPA and (bottom) DHA (as the respective FAMEs) from the algae harvested from Floway #1 (F1-diamonds), upper Floway #2 (F2U-X), and lower Floway #2 (F2L-triangles). Error bars represent the sample standard deviations of replicate derivatizations.

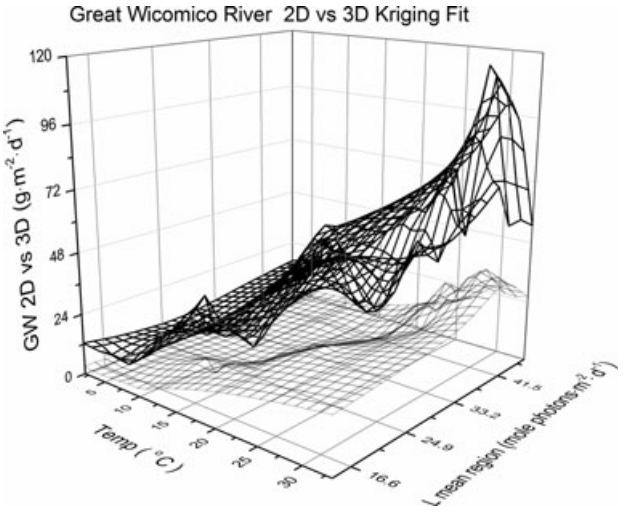

FIG. 6. Productivity of 3-D (#17) screen (bold) and combined 2-D screens (regular) as a function of temperature and light. The surfaces were fit with Kriging correlation using Origin 8.6 graphing.

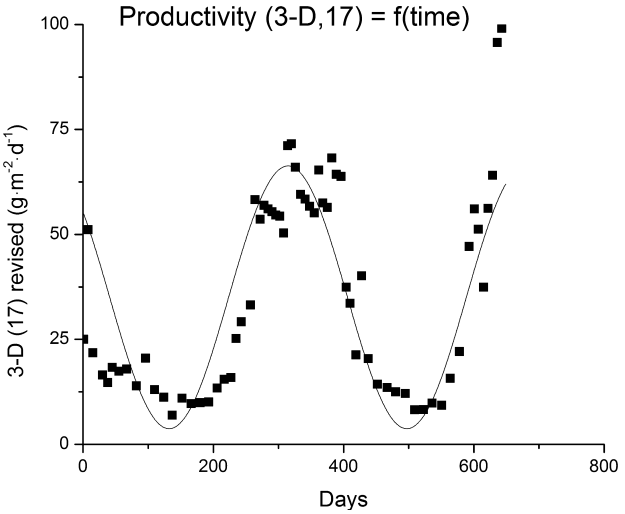

FIG. 8. Productivity of 3-D (#17) test screen as a function of time (estimated data have been substituted for six periods of harvest losses as described in the text). The line represents the empirical productivity function given by equation 2.

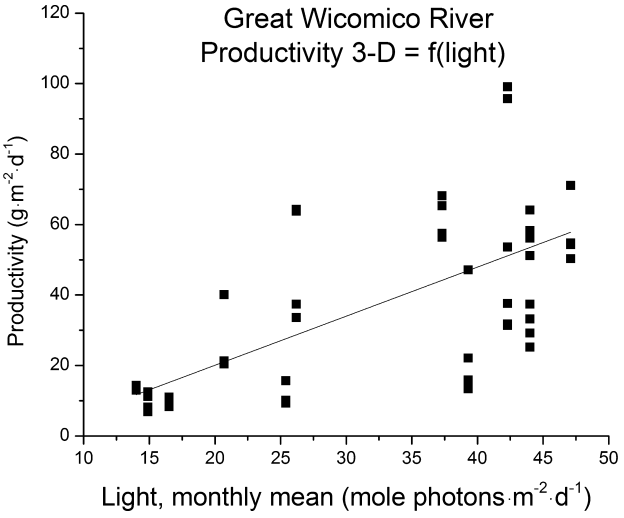

FIG. 7. Primary algal production on 3-D (#17) screen plotted against light. The line is a linear least-squares fit.

the river temperature at that time was 27°C. By mid-June, with no apparent reduction in production, and with water temperatures approaching 30°C, significant dips had not occurred. Mean yearly productivities on these floways were likely higher than those we presented earlier. Based on the hypothesis that occasional very high-temperature excursions on the ATS floways during the summer harvests in June and July 2010 caused artificially low measured biomass production, the annual mean and seasonal increase $P(t)$ may be even higher than the data (Fig. 2). For example, three harvests during the early summer of 2011 exceeded 90 $g \cdot m^{-2} \cdot d^{-1}$. Thus, the round-topped maroon curve shown in Figure 9, and derived from equation 2 with a higher P_t, provided the more likely representation of the production curve. In this case, the yearly mean production on 3-D substrates on ATS systems in the mid-Chesapeake Bay should be between 45 and 50 $g \cdot m^{-2} \cdot d^{-1}$ and the summer peak should be near 80 $g \cdot m^{-2} \cdot d^{-1}$. This would provide a significant increase in the efficiency of both nutrient removal and algal biomass production in ATS systems employed on non-point-source waters.

3-D screens were not only more productive than 2-D screens, they also provide an algal biomass with a higher organic and nutrient content (Table 2). While the difference in nutrient content was not large ($\Delta\%P \approx 20\%$; $\Delta\%N \approx 15\%$), with the greater productivity, the net nutrient removal was 3× that of the 2-D screens. With the temperature-compensated productivity demonstrated, the net nutrient removal was almost 4× larger.

The use of appropriately configured 3-D substrates allowed retention of diatom cells and filaments in the ATS environment, with its key element of moderated turbulence and mixing. Three-dimensional substrates also allowed greater packing of algal cells and therefore greater density of chl *a* and accessory pigments. These features were the key elements in maximizing algal photosynthesis and productivity in photobioreactors. In planktonic algal culture, the floating algal cells present an inherent impediment to cell packing, produce light-shading, and made constant exchange with the water around those cells difficult (Adey et al. 2011). In contrast, for cultures of benthic and other periphytic algal culture, ATS 3-D substrates provided numerous opportunities to increase productivity, with future engineering optimizing the key parameters that currently limit photosynthesis and production.

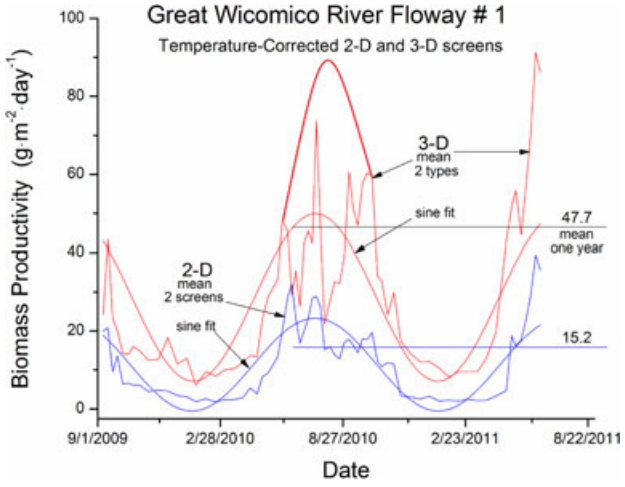

FIG. 9. Production curves of Figure 6, modified to fit equation 2 for summer production, assuming morning harvest to avoid lethal heating of residual floway algae during harvest. In this mode of operation, it is estimated that yearly mean biomass production at this location will be 47.7 $g \cdot m^{-2} \cdot d^{-1}$.

When diatoms were a significant component of biomass production on non-point-source ATS floways, production on 3-D substrates can be considerably enhanced. However, if nutrients were moderate to low in the incoming water, nutrient limitation (including CO_2 limitation) was possible down the floways (Table 1). If nitrogen removal was the target, shortening the floway, while maintaining total floway area, may lead to more economical removal. If phosphorus is the primary target, then longer floways with nitrogen injection may allow very high pH levels, with consequent phosphorus precipitation, providing the most economical operation (Craggs et al. 1996). Research has shown that the biochemically fixed Redfield ratio can range among taxa or can change depending on what type of macromolecules the alga is storing, or whether the nutrient is surface adsorbed (Geider and La Roche 2002, Sanudo-Wilhelmy et al. 2004). As demonstrated by the significantly higher P content in the downstream portion of Floway #2, phosphorus precipitation was likely occurring in the generally higher pH environment of the low part of the floways, especially the longer Floway #2 (Craggs et al. 1996). In any case, the lack of correlation between C, N, P, as noted earlier, suggests that the community growth was not N or P-limited, independent of carbon limitation.

Silicon dioxide is an essential nutrient for the metabolism and growth of diatoms, whose cell walls are composed of hydrated amorphous silica. Thus, diatom cell growth was highly coupled to ambient SiO_2 levels, as shown in several studies (Martin-Jézéquel et al. 2000, Claquin et al. 2002). Carbon and nitrogen levels in algae are specifically linked with photosynthesis. Since silicate is not directly coupled to photosynthesis, environmental factors such as incident radiation should not directly affect biomass SiO_2 levels. Although we hypothesize that the variation in composition could be due to algal species composition, terrigenous materials, making up roughly half of the silica, may be more important in the variability of silica content (Table 3). Thus, even though the total Si content was lower in winter when diatom relative abundance was maximum, the winter sample (23 February 2011) showed a higher proportion of biogenic silica than the summer sample did (23 May 2011) when Chlorophyta abundance was higher.

Being able to control the composition of the ATS algal communities will also be important for product application using the biomass as a feedstock. For example, oil-based biofuels (e.g., biodiesel) required high-lipid biomass to be economical and encouraging diatoms would be beneficial for biodiesel application. Specialized lipid products, such as PUFAs for nutritional supplements, may require species-specific accommodations. In contrast, for carbohydrate-based fuels like ethanol or butanol, communities dominated by Chlorophyta would likely be more useful. Regardless of the fate of the carbon-based component of the biomass, the nitrogen and phosphorus that are accumulated by the algal turf from the source water can be converted into appropriate fertilizer products. As demonstrated by Mulbry et al. (2008), the organic component also delays wash-out of nutrients, further enhancing the value of the fertilizer product.

One of the goals of this study was to assess the biofuel potential of ATS-grown algal biomass and compare it to other biofuel feedstocks. The USDA reports recent corn harvest averages of about 973 $g \cdot m^{-2} \cdot d^{-1}$ (155 $bu \cdot acre^{-1} \cdot year^{-1}$, USDA 2012), and an ethanol fermentation yield of 8.48×10^{-5} $L \cdot g^{-1}$ (2.76 $gal \cdot bu^{-1}$) for corn (USDA 2010). This translates to corn ethanol yields of 0.40 $L \cdot m^{-2} \cdot year^{-1}$. Corn is 66% starch (USDA 2010), which leads to a yeast fermentation ethanol yield of 1.28×10^{-4} $L \cdot g^{-1}$ of starch. Given the measured ~24% carbohydrate content of the biomass harvested from the Great Wicomico floways, and presuming equivalent ethanol yield from fermenting algal carbohydrates as from corn, we predict that an ATS installation with 3-D screens could produce about 2.24 $L \cdot m^{-2} \cdot year^{-1}$ ethanol, or about 5.6 times greater than for corn feedstock. Moreover, even the relatively low (~4%) lipid content of the algal turf biomass could produce 0.65$L \cdot m^{-2} \cdot year^{-1}$ of biodiesel, as compared to 0.055$L \cdot m^{-2} \cdot year^{-1}$ from soybeans, assuming recent U.S. harvests of 282 $g \cdot m^{-2} \cdot year^{-1}$ (42 $bu \cdot acre^{-1} \cdot year^{-1}$; USDA 2012), soy is 20.6 mass% oil, and an oil-to-biodiesel conversion efficiency of 82.4 mass% (USDA 2009). Algal turfs are thus superior to current terrestrial crops as feedstock for biofuel production.

Algal Turf Scrubber is the only significant, non-point-source technology for water quality amelioration in large watersheds. However, the area requirements of ATS are often cited as the single significant detrac-

tion. The high biofuel production capability created by use of 3-D substrates is critically important to ATS selection, since in many large watersheds vast acreage of corn and soy is planted for biofuels. Fertilization of these two crops is a major source of nutrients and hypoxia of waterways. Production of biofuels with ATS, coupled with nutrient removal, is a logical process for controlling nutrification and hypoxia.

Floway construction, operation, data collection, and algal analyses in this study were made possible by funding from HydroMentia, Ecological Systems Technology, The Lewis Foundation, Smithsonian Institution, and Statoil through the Virginia Institute of Marine Science. Chemical analyses were supported, in part, by funding from the U.S. Department of Energy (DE-FG3608GO88049), the Smithsonian Institution (T08CC10068), and the Virginia Institute of Marine Science (77263B/12683). We are grateful for discussions with Patrick Kangas of the University of Maryland, and Emmett Duffy and Elizabeth Canuel of the Virginia Institute of Marine Science. We thank the staff of InterfaceFLOR for their considerable efforts to simulate a manufactured version of the 3-D screen. E. Adey built the two floways studied, carried out many of the harvests, and participated in data analysis. J. Barker worked to provide excellent manuscript production.

Adey, W., Kangas, P. & Mulbry, W. 2011. Algal Turf Scrubbing: cleaning surface waters with solar energy while producing a biofuel. *Bioscience* 61:434–41.

Adey, W. & Loveland, K. 2007. *Dynamic Aquaria: Building and Restoring Living Ecosystems*, 3rd ed. Academic Press, Elsevier, 508 pp.

Adey, W., Luckett, C. & Jenson, K. 1993. Phosphorus removal from natural waters using controlled algal production. *Restor. Ecol.* 1:29–39.

Cade-Menun, B. & Paytan, A. 2010. Nutrient temperature and light stress alter phosphorus and carbon forms in culture-grown algae. *Mar. Chem.* 121:27–36.

Carpenter, R., Hackney, J. & Adey, W. 1991. Measurements of primary productivity and nitrogenase activity of coral reef algae in a chamber incorporating oscillatory flow. *Limnol. Oceanogr.* 36:40–9.

Cequier-Sánchez, E., Rodríguez, C., Ravelo, A. & Zárate, R. 2008. Dichloromethane as a solvent for lipid extraction and assessment of lipid classes and fatty acids from samples of different natures. *J. Agric. Food Chem.* 56:4297–303.

Chisti, Y. 2007. Biodiesel from microalgae. *Biotechnol. Adv.* 25:294–306.

Claquin, P., Martin-Jézéquel, V., Kromkamp, J., Veldhuis, M. & Kraay, G. 2002. Uncoupling of silicon compared with carbon and nitrogen metabolism and the role of the cell cycle in continuous cultures of *Thalassioria pseudonana* (Bacillariophyceae) under light, nitrogen and phosphorus control. *J. Phycol.* 38:922–30.

Conley, D. & Schelske, C. 1993. Potential role of spongespicules in influencing the silicon biogeochemistry of Florida lakes. *Can. J. Fish. Aquat. Sci.* 50:296–302.

Craggs, R., Adey, W., Jessup, B. & Oswald, W. 1996. A controlled stream mesocosm for tertiary treatment of sewage. *Ecol. Eng.* 6:149–69.

Dick, W. & Tabatabai, M. 1977. Determination of orthophosphate in aqueous solutions containing labile organic and inorganic phosphorus compounds. *J. Environ. Qual.* 6:82–5.

Geider, R. & La Roche, J. 2002. Redfield revisited: variability of C:N:P in marine microalgae and its biochemical basis. *Eur. J. Phycol.* 37:1–17.

Hessen, D., Færøvig, P. & Andersen, T. 2002. Light, nutrients, and P:C ratios in algae: grazer performance related to food quality and quantity. *Ecology* 83:1886–98.

Imbs, T. I., Shevchenko, N. M., Sukhoverkhov, S. V., Semenova, T. L., Skriptsova, A. V. & Zvyagintseva, T. N. 2009. Seasonal variations of the composition and structural characteristics of polysaccharides from the brown alga *Costaria costata*. *Chem. Nat. Compd.* 45:786–91.

Inhamuns, A. & Franco, M. 2008. EPA and DHA quantification in two species of freshwater fish from Central Amazonia. *Food Chem.* 107:587–91.

Laughinghouse, H. D. 2012. *Studies of Periphytic Algal Turf Scrubbers along the Chesapeake Bay: Community Structure, Systematic and Influencing Factors*. PhD dissertationUniversity of Maryland, College Park, 274 pp.

Martin-Jézéquel, V., Hildebrand, M. & Brzezinski, M. A. 2000. Silicon metabolism in diatoms: implications for growth. *J. Phycol.* 36:821–40.

Mulbry, W., Kondrad, S. & Pizarro, C. 2008. Treatment of dairy manure effluent using freshwater algae: algal productivity and recovery of manure nutrients using pilot-scale algal turf scrubbers. *Bioresour. Technol.* 99:8137–42.

Noseda, M. D., Siumara Tulio, S. & Duarte, M. E. R. 1999. Polysaccharides from the red seaweed *Bostrychia montagnei*: chemical characterization. *J. Appl. Phycol.* 11:35–40.

Potts, T., Du, J., Paul, M., May, P., Beitle, R. & Hestekin, J. 2011. The production of butanol from Jamaica Bay macroalgae. *Env. Progr. Sustain. Energy* 31:29–36.

Raven, D. & Beardall, J. 2003. Carbohydrate respiration and metabolism in algae. *In* Larkum, A. W. D., Douglas, S. E. & Raven, J. A. [Eds.] *Photosynthesis in Algae*. Academic Publishers, Dordrecht, Kluwer, pp. 205–8.

Reay, P. & Bennett, W. 1987. Determination of amorphous silica and total silica in plant materials. *Anal. Chim. Acta* 198:145–52.

Sandefur, H., Matlock, M., Costello, T., Adey, W. & Laughinghouse, H. D. IV 2011. Seasonal productivity of a periphytic algal community for biofuel feedstock generation and nutrient treatment. *Ecol. Eng.* 37:1476–80.

Sanudo-Wilhelmy, S., Tovar-Sanchez, A., Fu, F., Capone, D., Carpenter, E. & Hutchins, D. 2004. The impact of surface-adsorbed phosphorus on phytoplankton Redfield stoichiometry. *Nature* 432:897–901.

Singh, A. & Olsen, S. I. 2011. A critical review of biochemical conversion, sustainability and life cycle assessment of algal biofuels. *Appl. Energy* 88:3548–55.

Skriptsova, A. V., Shevchenko, N. M., Zvyagintseva, T. N. & Imbs, T. I. 2010. Monthly changes in the content and monosaccharide composition of fucoidan from *Undaria pinnatifida* (Laminariales, Phaeophyta). *J. Appl. Phycol.* 22:79–86.

Stewart, A. 2006. *Preliminary Engineering Assessment for a Comprehensive Algal Turf Scrubber Based Nutrient Control Program for the Suwannee River in Florida*. Suwannee River Water Management District, Live Oak, FL, 18 pp. 18 Sheets.

USDA. 2009. Energy life-cycle assessment of soybean biodiesel. (Agricultural Economic Report Number 845). Available at: http://www.usda.gov/oce/reports/energy/ELCAofSoybeanBiodiesel91409.pdf (last accessed 05 December 2012).

USDA. 2010. 2008 Energy balance for the corn-ethanol industry. (Agricultural Economic Report Number 846). Available at: http://www.usda.gov/oce/reports/energy/2008Ethanol_June_final.pdf (last accessed 05 December 2012).

USDA. 2012. National Agricultural Statistics Service: Charts and Maps – Field Crops. Available at: http://www.nass.usda.gov/Charts_and_Maps/Field_Crops/index.asp (last accessed 07 November 2012).

Utermöhl, H. 1958. Zur Vervollkommnung der quantitativen Phytoplankton-Methodik. *Mitt. Int. Ver. Limnol.* 9:1–38.

Wang, B. & Lan, C. 2011. Biomass production and nitrogen and phosphorus removal by green alga *Neochloris oleobundans* in simulated wastewater and secondary municipal wastewater effluents. *Bioresour. Technol.* 102:5639–44.

Supporting Information

Additional Supporting Information may be found in the online version of this article at the publisher's web site:

Appendix S1. Sources and preparation of the materials, reagents and samples used for chemical analysis of the ATS biomass.

Figure S1. Surging device at the input of Floway #1. This dump-trough, mounted on a single nylatron rod axis, fills with water and dumps approximately every 30 s, providing an oscillatory flow in the ATS floway. Note the dense buildup of diatom biomass (primarily *Berkeleya*) on the floway.

Figure S2. Floway #1 during the spring of 2011. At this time a mix of *Ulva intestinalis*, *Berkeleya rutilans*, and *Ulothrix* sp. dominated the floway with dense, stringy masses.

Figure S3. Hand-woven 3-D growth substrate (vertical, braided fibers attached at the nodes of a 5 mm mesh, spiral-wound, basal screen) overlying the "standard" 2-D, 2 × 5 mm mesh screen.

Figure S4. Temperature of the Great Wicomico River at the ATS water intakes, and the discharge temperature of Floway #1.